RSC Advances

ROYAL SOCIETY OF CHEMISTRY

www.rsc.org/advances

Non-steady state migration of chloride ions in cement pastes at early age

S. W. Tang*, Z. J. Li, E. Chen, H. Y. Shao

Department of Civil and Environment Engineering,
The Hong Kong University of Science and Technology,
Kowloon, Clear Water Bay, Hong Kong

* Corresponding Author:
E-mail: tangshengwen1985@163.com

Tel: +852-68794395
Fax: +852-23581534

Abstract

This paper proposes a preliminary work to study the diffusion and migration of chloride ions in cement pastes at early age. The non-steady state ion migration coefficients of cement pastes are evaluated from three aspects: 1) electrical rapid ion migration test; 2) non-contact impedance measurement (NCIM) based on a fractal model; and 3) a corresponding simulation of "I" shape fractal network. The experimental results from electrical rapid ion migration test and NCIM have good agreement. The influences of water to cement ratio, curing hydration age and addition of mineral admixtures on performance of ion diffusion/ migration in cement pastes are investigated.

Keywords: Ion diffusion/migration; Electrical rapid ion migration; Impedance; Fractal network; Cement paste; Steady state; Early age; Pore structure; Hydration; Fractal

1. Introduction

The durability of cement-based materials, the most used artificial material, is a fundamental topic in many construction engineering fields; it is imperative to understand the durability characteristics of cement-based materials in order to facilitate its use in all kinds of aggressive environments[1]. One of key evaluation indices of durability is referred to as ion diffusion/migration resistance in cement-based materials. Ion diffusion/migration is considerably significant for the heat and mass transfer in cement-based materials[1]. In general, there are several diffusion/ migration coefficients frequently mentioned for the study of transportation performance in cement-based materials [2, 3], i.e. D_{ssd} the steady state diffusion coefficient; D_{ssm} the steady state migration coefficient; D_{nssd} the non-steady state diffusion coefficient; D_{nssm} the non-steady state migration coefficient. Until now, the key relation between D_{ssd} and D_{nssm} is not yet completely developed in cement-based materials at early age. D_{ssd} may be the most important parameter for characterization of transportation, which is primarily influenced by intrinsic pore structure of cement-based materials; the steady state diffusion takes place at a constant rate and is independent of flow diffusion distance and time. Nevertheless, the steady-state tests are always not preferred from the practical view as they are extremely time consuming and laborious [4]. Instead, the electrical rapid ion migration test has been developed to overcome these drawbacks. The rapid ion migration method performed in this work is an accelerated method which assesses the ion penetration resistance according to the electrical charge passing through cement-based materials in the first several hours of the test [5].

On the other hand, some recent studies demonstrate that electrical impedance approaches coupled with sophisticated circuits modeling have the potential to study the evolution of steady state ion diffusion, pore structure and permeability cement-based materials non-destructively in real time [6-10], and hence, if ion binding capacity inside the cement-based materials is considered, it is possible to derive the evolution of non-steady state migration coefficients of cement-based materials.

Besides, it has been proved that most of real porous media present fractal performance in nature and a realistic picture of disordered porous system could be provided by a fractal description [11]. In particular, it has been found that cement-based materials are such kind of typical fractal porous media as well [8]. Therefore, another alternative evaluation method for non-steady state ion migration coefficients is recently promoted fractal network simulation, apart from electrical migration test and impedance measurement [12-14]; such simulation is likely to intuitively study the influence of all kinds of pore parameters on non-steady state ion migration of cement-based materials.

In this work, the aggressive ion in this work is considered as chloride ion commonly-available in a marine environment[1]. The influence of water to cement ratio, hydration age and mineral admixture (fly ash, slag and silica fume) of cement pastes on the performance of ion diffusion/migration are clarified. The non-steady state migration coefficients $\left(D_{nssm}\right)$ of cement pastes are determined by electrical rapid ion migration method and a newly-proposed non-contact impedance measurement (NCIM) based on a fractal model; exact relation between pore structure and non-steady state chloride migration property in fractal saturated cement pastes is well established. A corresponding simulation of "I" shape fractal network is

73 further proposed to study the influence of porosity and pore size of network on non-steady
74 state ion migration of fractal cement pastes.

75 2. Experiments and Methods

76 *2.1 Materials and mix proportion*

77 In this work, ordinary Portland cement meeting the requirement of ASTM Type I and de-air
78 and de-ion water were used. Cement pastes with water to cement ratios (w/c) 0.3, 0.4 and 0.5
79 by mass were prepared and marked as P3, P4 and P5. Cement pastes with notations of F10,
80 F20, F30 and F40 were also prepared. F10, F20, F30 and F40 represented pastes with water to
81 binder (cement+ mineral admixture) ratio (w/b) of 0.4, in which 10, 20, 30 and 40% of
82 cement were replaced by fly ash by mass. Similar, S10, S30, S50 and S70 denoted that 10, 30,
83 50 and 70% of cement were replaced by slag and w/b ratios were 0.4. SF5 and SF10 with w/b
84 ratio 0.4 meant that 5% and 10% of cement were replaced by silica fume, respectively. These
85 fresh pastes were prepared in a planetary-type mixer at 45 rpm for 2 minutes first and then at
86 90 rpm for 2 minutes. The chemical compositions of the cement, fly ash, slag and silica fume
87 are given in Table 1. The morphology of cement, fly ash, slag and silica fume observed by a
88 JEOL 6300 scanning electron microscope (SEM) is shown in Figure.1.

89 **Table 1** The chemical composition of cement, fly ash, slag and silica fume (wt%)

Cement	CaO	SiO_4	Fe_2O_3	Al_2O_3	SO_4	MgO	K_2O	TiO_2	LOI
wt%	61.12	18.71	6.11	5.92	3.55	3.08	0.22	0.09	1.2

Fly ash	SiO_2	Al_2O_3	TiO_2	CaO	Fe_2O_3	Na_2O	P_2O_5	SO_4	K_2O	MgO	MnO	LOI

wt%	50.26	30.11	3.82	3.26	3.17	2.11	1.72	1.25	1.02	1.01	0.06	2.12
slag	SiO_2	CaO	Al_2O_3	MgO	SO_4	TiO_2	K_2O	MnO	Fe_2O_3	LOI		
wt%	38.47	36.92	10.02	5.52	4.63	1.01	0.52	0.38	0.19	2.34		

Silica fume	SiO_2	K_2O	CaO	SO_4	MgO	MnO	Fe_2O_3	LOI
wt%	92.39	2.63	1.21	0.99	0.61	0.19	0.16	1.82

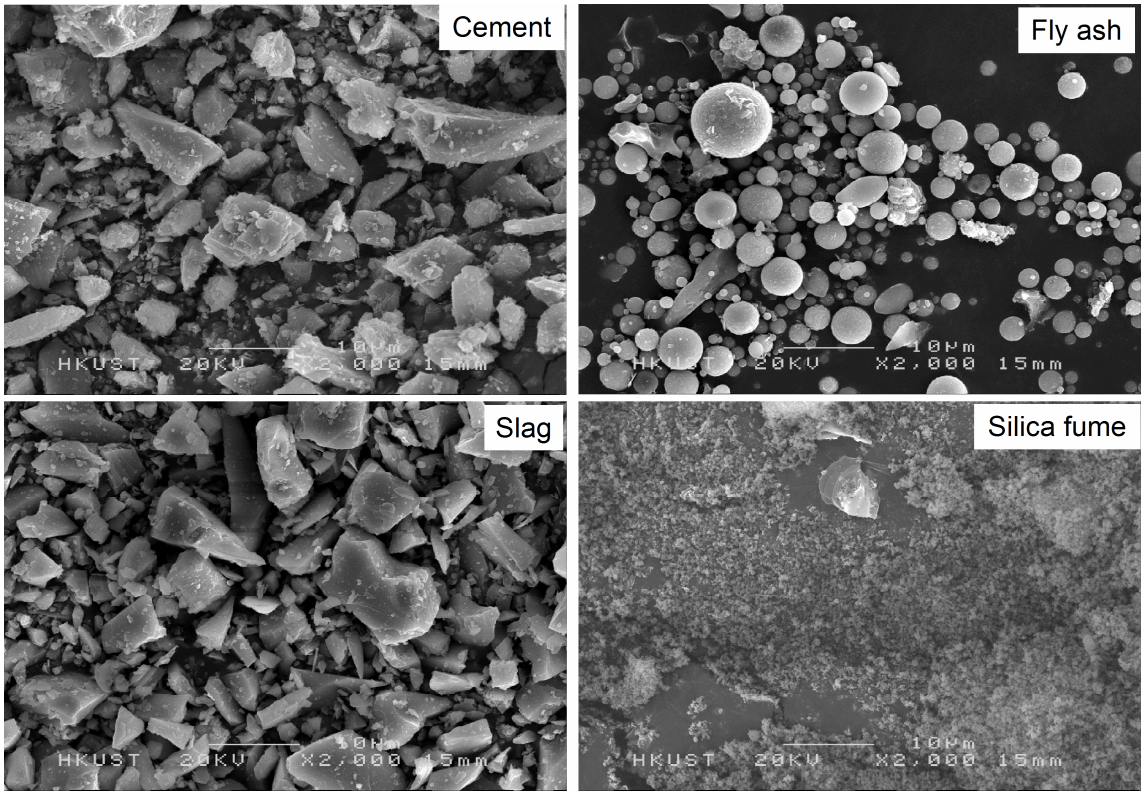

Fig.1. Morphology of cement, fly ash, slag and silica fume

2.2 Experimental tests

2.2.1 Non-contact impedance measurement

NCIM without electrodes can record the electrical impedance of cement pastes non-destructively in-situ during the whole hydration process[8]. A series of resistor-capacitor and resistor-inductor series circuits have been used to inspect the accuracy of NCIM: the measured impedance response can be perfectly coincident with the ones calculated by corresponding nominal values. The working mechanism and corresponding test procedure of NCIM can be consulted in Ref.[8]. The tests were implemented in the environmental chamber with temperature (20℃) and humidity (100%) for 3 days.

2.2.2 Compressive strength test

The fresh cement pastes were cast into 4cm×4cm×4cm moulds for compressive strength tests at 1 day and 3 days. The tests were undertaken with a loading rate 1kN/s.

2.2.3 Electrical rapid ion migration

In the present study, the electrical rapid ion migration (ERIM) test and procedure similar to those described in ASTM 1202-05 were employed, as shown in Figure 2. The cement pastes at hydration age 1 and 3 days were in cylindrical shape (100mm in diameter and 50mm in thickness) [6]. The tests were performed onto cement pastes through mesh brass at a voltage of 4V for four hours to avoiding the excessive temperature increase. After ERIM test, the cylindrical cement pastes were split into two halves. Colorimetric method was applied to find the depth of chloride penetration (x) by spraying a 0.1 N $AgNO_3$ solution on the exposed surface [6]. Three identical cement pastes were prepared in order to gain the average value of non-steady state migration coefficient. The non-steady state migration coefficient (D_{nssm}) for each cement paste is determined by this test from Eq.(1):

$$D_{nssm} = RT/\left(|z|FEt\right)\left[x - 2erf^{-1}\left(1-2C_d/C_0\right)\cdot\sqrt{x}/\sqrt{|Z|FE/(RT)}\right] \quad (1)$$

where z is the electrical charge of ion which is equal to -1 for chloride; F is the Faraday constant(=96480 coulomb/mole); E is the strength of electric field, which is the voltage per unit length between anode and cathode; R is the universal gas constant, 8.314 J/(mol·K); T is absolute temperature in the environment, 293.15K; $erf^{-1}(x)$ is the inverse error function; C_d is the concentration of ion at distance x from the surface, is taken as 0.07N; C_0 is the ion concentration at the surface of the cement paste and taken to be 0.5N; t is test time.

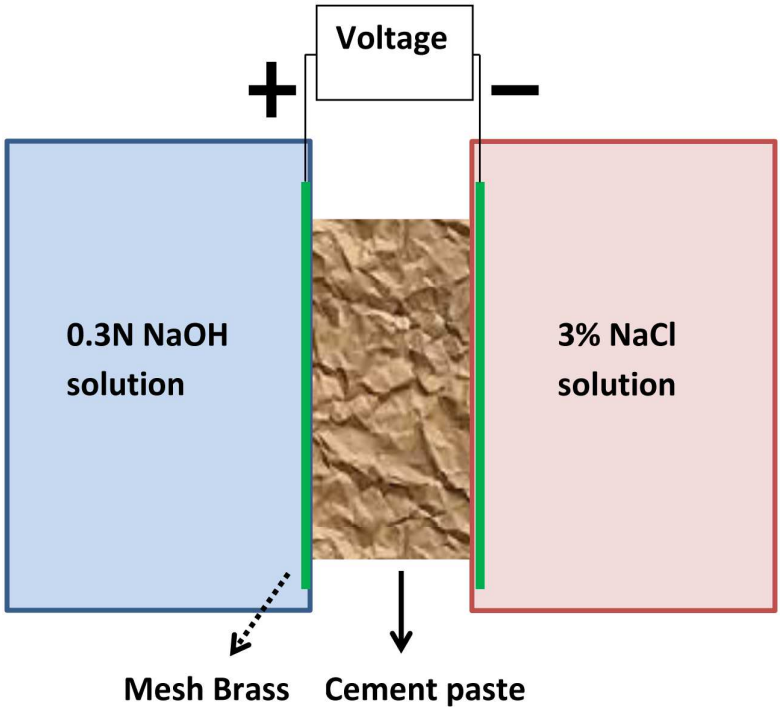

Fig.2. Illustration of electrical rapid ion migration test

3. Non-steady state migration coefficient predicted by NCIM

In this work, a fractal model with the aid of NCIM is developed to study the non-steady state migration coefficient of fractal saturated cement pastes. First of all, the effective diffusion coefficient (D_s) in the pore solution of saturated cement paste is given as [3,15]:

$$D_s = D_{-0}\left(1 - zK_{\tau 0}\right)\left(1 + \frac{\partial \ln \gamma}{\partial \ln c}\right)\frac{2c + c_0}{f\left(1 - |\beta_v|\right)c + c_0} \tag{2}$$

where D_{-0} is the diffusion coefficient of anions in the infinite dilute solution, equal to 2.03×10^{-9} m^2/s [15]; $K_{\tau 0}$ is the difference in transference number in the external source solution, whose typical value is $-0.207\times10^{-8}\,m^2\cdot s\cdot V$ [15]; γ is the activity coefficient of ions in pore solution; c is the free chloride concentration of ions in the pore solution; $\partial \ln \gamma / \partial \ln c$ is determined as -0.025 L/mol [15]; c_0 is the solvent concentration, approximately equal to 56.45 mol/L[16]; f is the friction coefficient which reflects the ionic interaction in the pore solution, predicted as 15000 by Tang et al [16]; β_v is the ratio of cation velocity to anion velocity and equal to 0.427 [16].

The mass flow rate of ion diffusion $(q(d))$ in a single tortuous pore path for fractal cement pastes is derived as [17]:

$$q(d) = D_s A(d)\Delta c / L_t(d) = D_s A(d)\Delta c / \left(d^{1-D_t} L_0^{D_t}\right) \tag{3}$$

where $A(d)$ is the cross sectional area of pore channels with diameter d; Δc is the concentration difference between two ends of pore channels; $L_t(d)$ is the actual length of pore

146 channel, which is satisfied with classical fractal law [9]; L_0 is the measured length of cement
147 paste; D_t is the fractal dimension associated with pore tortuosity.
148 Meanwhile, the number of pore size (δN) between d and $(d+\delta d)$ in fractal cement paste
149 and cross-section area of the saturated cement paste (A_t) are [9, 17]:

150 $$-\delta N = D_f d_{\max}^{D_f} d^{-D_f-1}\delta d \tag{4}$$

151 $$A_t = -\frac{1}{\phi}\int_{d_{\min}}^{d_{\max}} \frac{1}{4}\pi d^2 \delta N = \frac{\pi D_f}{4\phi\left(2-D_f\right)} d_{\max}^{D_f}\left(d_{\max}^{2-D_f} - d_{\min}^{2-D_f}\right) \tag{5}$$

152 where D_f is the fractal dimension fore pore space; $d_{\max}$ and $d_{\min}$ are maximal and minimal
153 pore diameters in saturated cement paste; ϕ is the porosity of a cement paste.
154 The total mass flow rate $(Q(d))$ and steady state diffusion coefficient (D_{ssd}) predicted by
155 NCIM are expressed as [17]:

156 $$Q(d) = -\int_{d_{\min}}^{d_{\max}} q(d)\delta N = \frac{\pi D_s \Delta c D_f d_{\max}^{D_f}}{4L_0^{D_t}\left(D_t - D_f + 1\right)}\left(d_{\max}^{D_t-D_f+1} - d_{\min}^{D_t-D_f+1}\right) \tag{6}$$

157 $$D_{ssd} = Q(d)L_0/\left(A_t\cdot\Delta c\right) = \frac{D_s L_0^{1-D_t}\phi\left(2-D_f\right)\left(d_{\max}^{D_t-D_f+1} - d_{\min}^{D_t-D_f+1}\right)}{\left(D_t - D_f + 1\right)\left(d_{\max}^{2-D_f} - d_{\min}^{2-D_f}\right)} \tag{7}$$

158 With respect to Eq.(7), L_0 can be measured when the NCIM test is completed; $d_{\min}$ is
159 predicted as 6.2nm from electrical double layers model [8]; ϕ , D_f , D_t and $d_{\max}$ can be
160 determined from NCIM [8,9].
161 With the purpose of verification, the predicted D_{ssd} of fractal saturated cement paste from a
162 fractal model by means of NCIM will further transfer to D_{nssm} in order to compare the

163 relevant result from ERIM. The transformation relation between D_{ssd} and D_{nssm} is studied by
164 Tang et al through transformation ratio, T_r [3, 15, 16]:

165 $$D_{ssd}/D_{nssm} = T_r = \left(1 - zK_{\tau 0}\right)\left(1 + \frac{\partial \ln \gamma}{\partial \ln c}\right)\frac{f\left(1+\left|\beta_v\right|\right)c + c_0}{f\left(1-\left|\beta_v\right|\right)c + c_0}\left(\phi + \partial C_b/c\right)\Big/\left[1 + \left(\frac{1}{a}\frac{\partial c}{\partial x} + c\right)\frac{a}{\partial c}\right] \quad (8)$$

166 $$a = -\frac{zK_{\tau 0}}{c}\left(1 + \frac{\partial \ln \gamma}{\partial \ln c}\right)\frac{\partial c}{\partial x} \quad (9)$$

167 where C_b is the bound chlorides with the dimension of kg Cl^-/m^3; the term $\partial C_b/c$ mainly
168 reflects chloride binding capacity in the fractal cement paste and can be derived from Eq.(10)
169 and (11) [18,19] although Spiesz and Brouwers considered that this binding capacity may be low
170 to some extent [4].

171 $$\partial C_b/\partial c = \frac{\alpha(t)k_h^m}{w/c + 1/D_c}\cdot\left(0.345\cdot c^{-0.666} + 0.512\cdot c^{-0.421}\right) \quad (10)$$

172 $$\alpha(t) = \left[\frac{w/b}{D_w} - \phi\cdot V_{total}\right]\cdot\frac{D_c D_h}{D_c - D_h} \quad (11)$$

173 where $\alpha(t)$ is hydration degree of cement pastes; k_h^m is the total mass of the hydration
174 products as 1 gram of cement is totally hydrated, taken as 2.06 g/g[19]; w/b is water to binder
175 ratio of cement pastes; D_w, D_c and D_h are density of water (1.01 g/cm^3), cement (3.15 g/cm^3)
176 and hydrated products (1.529 g/cm^3) [18]; V_{total} the total volume of cement pastes, which can be
177 measured after NCIM test is completed [18].

178 Actually, it is also worth pointing out that the application of this fractal model to predict the
179 non-steady state ion migration coefficient is not only restricted for the case of fractal saturated
180 cement paste. This model may be possibly used in other cases of fractal porous media, such as

melt crystallization of porous crystal layer [20], diffusion-controlled reaction of fractal porous electrodes [21], if the fractal dimensions, ion binding capacity, minimal and maximal pore diameters are determined from either simulation or experimental techniques.

4. Non-steady state migration simulation

In this work, a fractal simulation based on an "I" shape network is also developed to analyze non-steady state migration coefficients in fractal saturated cement pastes. Figure 3 is the two dimensional configuration of fractal "I" shape network in the cuboid of saturated cement paste. This figure only lists this network to Step 2 with the purpose of simplicity.

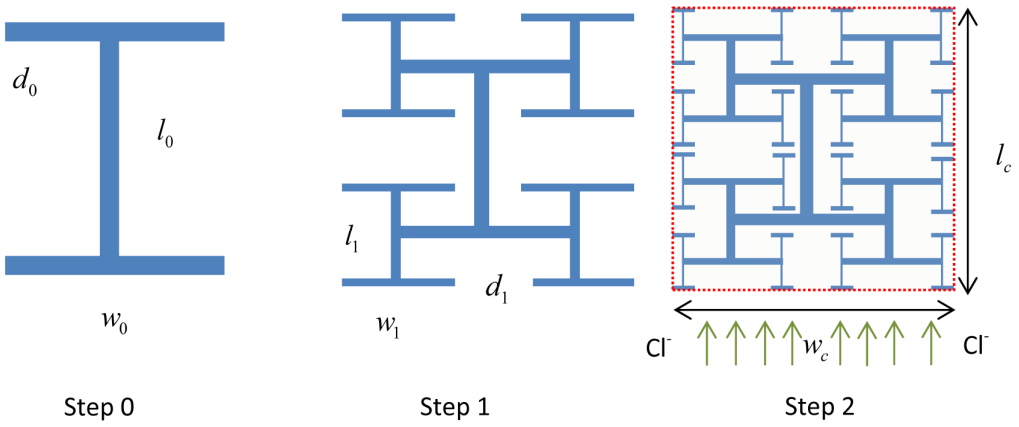

Fig.3. Configuration of "I" shape network in the cuboid of saturated cement paste

This "I" shape network proposed originates from the largest mother "I" channel with circular cross section. This mother channel extends four symmetrical "I" channels further in subsequent step. The similar construction procedure is then implemented continuously to each new "I" channel ad infinitum. This network echoes actual pore size distribution in cement

196 pastes since the fraction of number of small pores in entire pore range usually takes a great
197 portion in the media and vice versa [9]. First of all, the basic assumptions of "I" shape network
198 are described as [22]:1) each channel in the network is straight and smooth; and 2) the thickness
199 of electrical double layers of pores, approximately 2.18 nm, is not taken into account [8].

200 As illustrated in Figure 3, the size of largest mother "I" channel in Step 0 has width w_0 ,
201 diameter d_0 and vertical length l_0. w_k, w_{k-1}, d_k, d_{k-1} l_k and l_{k-1} are accordingly width, diameter
202 and vertical length of "I" channel in Step k and $k-1$. The relations of these dimensional
203 parameters in adjacent steps are defined by several scale factors α, β and γ as [12]:

204 $$\alpha = w_k / w_{k-1} \tag{12}$$

205 $$\beta = d_k / d_{k-1} \tag{13}$$

206 $$\gamma = l_k / l_{k-1} \tag{14}$$

207 It should be noted that the "I" shape network is embedded in particular cuboid which
208 represents a saturated cement paste. The red dash line box shown in Figure 3 stands for such
209 cuboid, which has width w_c, length l_c and thickness d_0. w_c and l_c can be determined from
210 Eq.(15) and (16), respectively; the effective porosity (ϕ_c) of cuboid can be also deduced
211 further when the step of "I" shape network is equal to k [12]:

212 $$w_c = w_0 + w_1 + w_2 + \cdots + w_k = w_0 \left(1-\alpha^{k+1}\right) \Big/ \left(1-\alpha\right) \ \ (k \geq 0) \tag{15}$$

213 $$l_c = l_0 + l_1 + l_2 + \cdots + l_k + 2d_k = l_0 \left(1-\gamma^{k+1}\right) \Big/ \left(1-\gamma\right) + 2d_0\beta^k \ \ (k \geq 0) \tag{16}$$

214 $$\phi_c = \frac{\frac{\pi d_0 l_0}{4}\left[1+\frac{4\beta^2\gamma-\left(4\beta^2\gamma\right)^{k+1}}{1-4\beta^2\gamma}\right]+\frac{\pi d_0 w_0}{2}\left[1+\frac{4\beta^2\alpha-\left(4\beta^2\alpha\right)^{k+1}}{1-4\beta^2\alpha}\right]}{L_c w_c} \quad (k\geq 0) \tag{17}$$

215 The number of "I" channel, whose diameter is not less than d_k, can be calculated from key

216 fractal scale law as [8]:

217 $$1+4+4^2+\cdots+4^k=\left(d_0/d_k\right)^{D_f}=\beta^{-kD_f}=\left(4^{k+1}-1\right)/3 \quad (k\geq 0) \tag{18}$$

218 In addition, the chloride penetration direction to the cuboid is demonstrated in Figure 3. The

219 effective concentration gradient per unit length $\left(\Delta c_u\right)$ along the penetration direction is

220 defined as:

221 $$\Delta c_u=\Delta c/\left(l_0+l_1+l_2+\cdots+l_k\right)=\frac{\Delta c\left(1-\gamma\right)}{l_0\left(1-\gamma^{k+1}\right)} \quad (k\geq 0) \tag{19}$$

222 With regard to steady state diffusion case, the total mass flow rate through the saturated

223 cement paste $\left(Q_t\right)$ is equal to that through "I" shape network, as shown in Eq.(20); thereupon,

224 the formula of steady state diffusion coefficient of "I" shape network $\left(D_{ssd}^{net}\right)$ is also presented

225 as[17]:

226 $$Q_t=D\Delta c_u\frac{\pi d_0^2}{4}\frac{1+2\beta^2-2^{k+2}\beta^{2k+2}}{1-2\beta^2} \quad (k\geq 0) \tag{20}$$

227 $$D_{ssd}^{net}=Q_t l_c/\left(A_t\Delta c\right)=Q_t l_c/\left(w_c d_0\Delta c\right)=D\frac{1-\gamma}{l_0\left(1-\gamma^{k+1}\right)}\frac{\pi d_0 l_c}{4w_c}\frac{1+2\beta^2-2^{k+2}\beta^{2k+2}}{1-2\beta^2} \quad (k\geq 0) \tag{21}$$

228 When the ion binding capacity is taken into account, eventually, non-steady state migration

229 coefficient of "I" shape network $\left(D_{nssm}^{net}\right)$ is given as:

$$D_{nssm}^{net} = D_{ssd}^{net} / \langle T_r \rangle \quad (22)$$

where $\langle T_r \rangle$ is average experimental transformation ratio among cement pastes.

In this work, the influences of porosity and pore size on non-steady state ion migration in fractal saturated cement paste are evaluated by a simulation based on "I" shape network. The algorithm for this simulation is concluded as follows:

1) Determine the diffusion coefficient of ion (D_s) in the infinite dilute solution from Tang's work [15].

2) Set the average transformation ratio $(\langle T_r \rangle)$ from experiments.

3) Select the appropriate porosity of the cuboid, sizes of largest mother channel and step number of "I" shape network, viz., ϕ_c, d_0, w_0, l_0 and k.

4) A set of D_f between 1 and 2 is produced randomly [9].

5) Calculate the average value of non-steady state migration coefficient of "I" shape network $(\langle D_{nssm}^{net} \rangle)$ and corresponding variance (σ) using Eq.(21),(22) and (23).

$$\sigma = \sqrt{\langle D_{nssm}^{net\ 2} \rangle - \langle D_{nssm}^{net} \rangle^2} \quad (23)$$

where $\langle D_{nssm}^{net\ 2} \rangle$ is the average of square of non-steady state migration coefficient of "I" shape network.

5. Results and discussion

5.1 Electrical rapid ion migration

Figure 4 is non-steady state migration coefficient of cement pastes at hydration age 1 day and 3 days measured by electrical rapid ion migration. In this figure, pastes with higher water to cement ratio, dosage of fly ash or slag usually exhibit larger values of non-steady state chloride migration coefficient. In the case of higher water to cement ratio, less solid phases exist in the paste, volume of the pore space or channels for ion transportation in cement pastes can be thus larger, which can bring about larger ion migration value to great extent[1]. Pozzolanic reaction of fly ash or slag does not occur until the certain amount of calcium hydroxide is generated in blended cement pastes, early hydration and formation of pore structure skeleton will be retarded when fly ash or slag are added into cement pastes[1, 23], and hence, the resistances to ion transportation of fly ash/slag blended pastes are smaller than those of pure pastes at early hydration stage. With regard to silica fume case, pastes with higher silica fume dosage in turn exhibit lower values of non-steady state chloride migration coefficient. As silica fume composed of small particles is mixed with water and immediately covered by a gel-like layer[23], this may result in a rapid percolation of solid phase and formation of initial pore skeleton. Longer hydration age is also beneficial to reduction of non-steady state chloride migration coefficient since more hydrated products are filled into pore space [24].

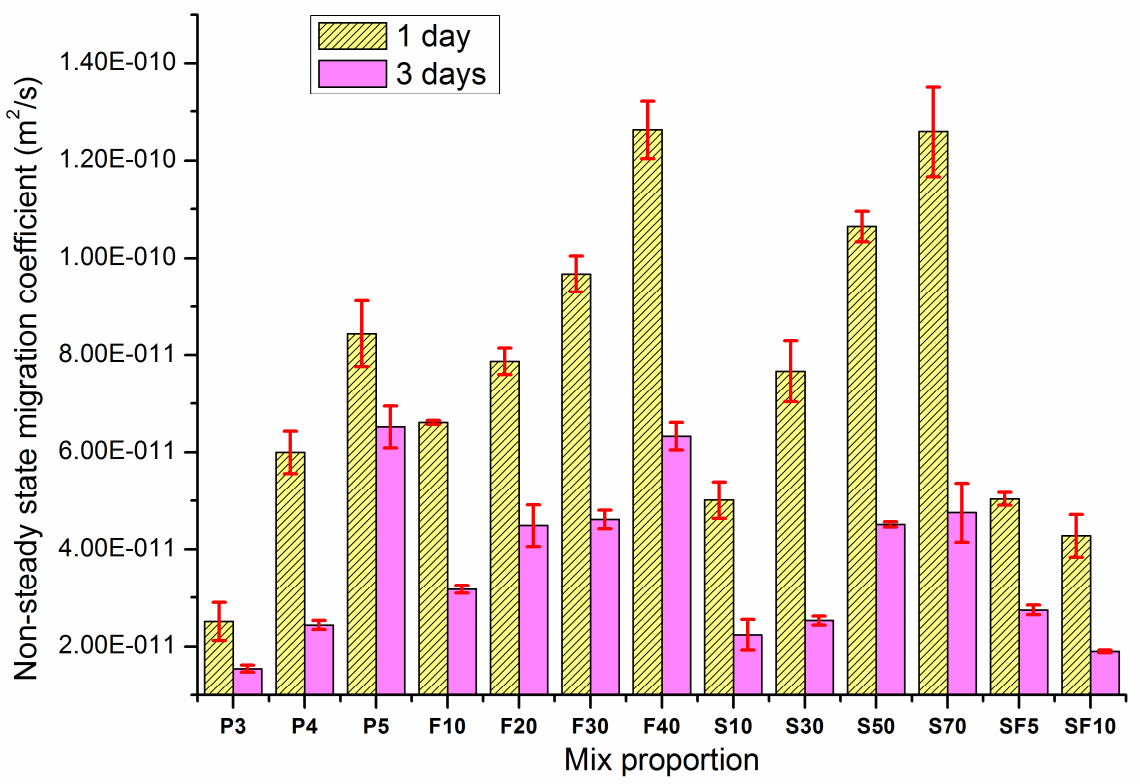

Fig.4. Non-steady state migration coefficient measured by electrical rapid ion migration

For further validation, compressive strength values of cement pastes at hydration age 1 and 3 days are presented in Figure 5. Strength development in cement pastes primarily depends on the increase of hydration degree or decrease of pore volume [18]. In principle, cement pastes with low ion diffusion/migration ability usually exhibit superior high compressive strength values[1], it is confirmed that results in Figure 5 correspond to ones presented in Figure 4.

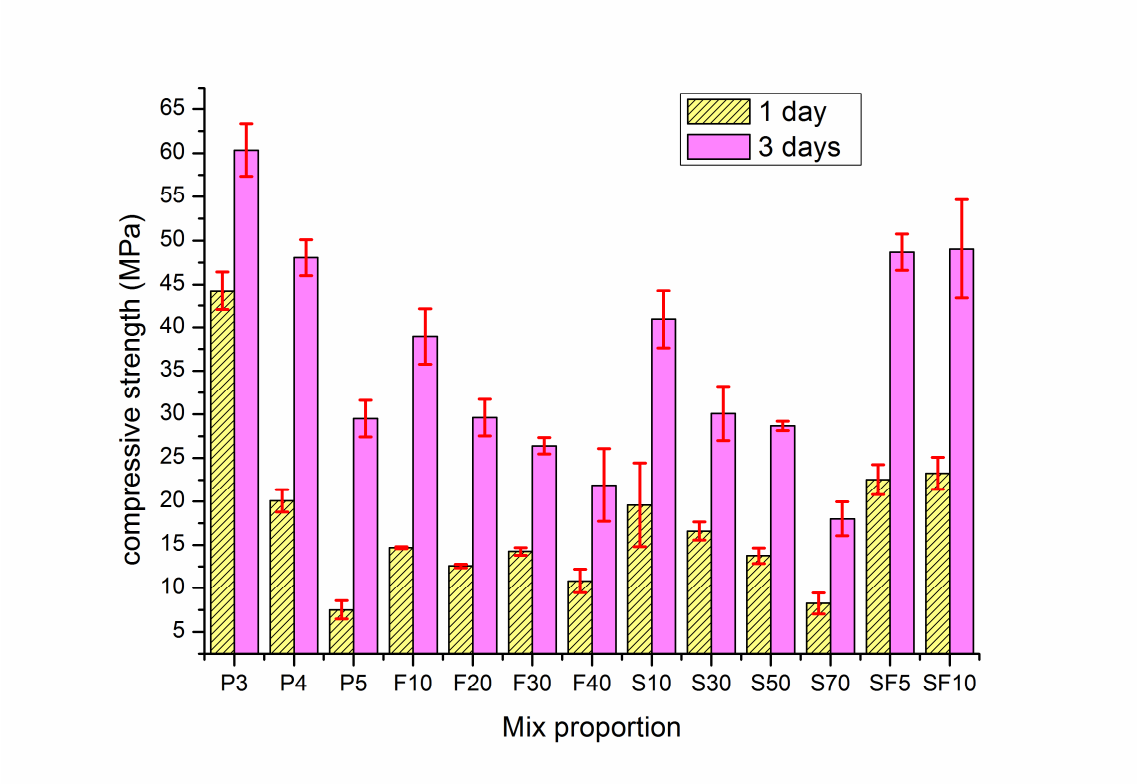

Fig.5. Compressive strength of cement pastes at hydration age 1day and 3days

5.2 Comparison of non-steady state migration coefficients

It may be instructive to compare results either measured from ERIM test in this work or previous literatures, or predicted from the fractal model mentioned above to check merits inherent with the application of each method. It is unfortunate few of experimental electrical migration results for young cement pastes in previous literatures are found since considerably long test time of electrical migration measurement is indispensable [6]. The comparison of measured and predicted non-steady state migration coefficients of saturated cement pastes from ERIM test and fractal model is shown in Figure 6. On the whole, it can be clearly seen that most of data sets of saturated cement paste have good agreement at hydration age 1 and 3

285 days, respectively. The minor differences between measured and predicted results in Figure 6
286 may be rooted in several factors: 1) Of particular note is that the mobility of ion migration
287 may be accelerated since a high temperature is inevitably generated during the ERIM test
288 when an electrical voltage is applied on sides of cement pastes [25]; moreover, the replacement
289 of Na^+ and OH^- ions with Cl^- in the pore solution of cement pastes may induce some
290 microstructural changes by formation of new amorphous solid products either within the
291 pores or as electrochemical double layers along the pore walls during ERIM test [6]; 2) The
292 derivation of non-steady state migration coefficient from the proposed fractal model based on
293 NCIM is a bit complex and involves so many parameters; although how to derive these
294 parameters has been already explained in detail by Tang et al through a pure solution system
295 or solution-concrete system [3,15,16], the pore solution in cement pastes is not actual pure
296 solution, and proved as mixed-solvent electrolyte solution [4]. The contribution of individual
297 species and interactions between pairs of species to ion transportation may be seriously
298 considered in the prediction of non-steady state migration coefficient via fractal model [4].
299 However, it may be somewhat difficult to determine these actual contributions of ions
300 constrained by pore structure to the effective diffusion coefficient (D_s) in the complex
301 interconnected pore network of cement pastes with hydration until now [4,8]; 3) Hydration and
302 microstructure of fresh cement pastes develop quickly and necessary test time is usually
303 required in ERIM test [1] ; for these cases, test timings between ERIM and NCIM may not
304 coincide completely; and 4) Assumptions inherent with the application of different techniques
305 for ion migration, for instance, neglected diffusion flux during ERIM test [4] and the empirical
306 prediction of minimal and maximal pore diameters in the fractal model [8,9], may be one of
307 sources of scattered results in Figure 6 [9,24].

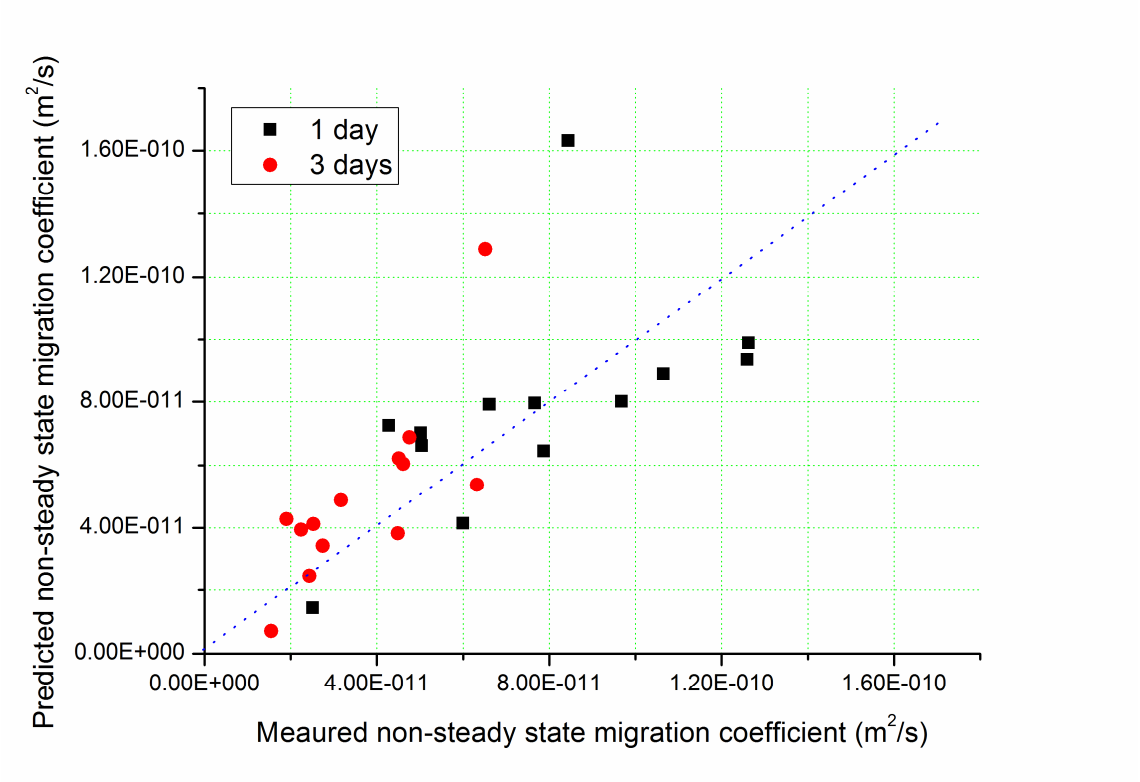

Fig.6. Comparison of measured and predicted non-steady state migration coefficients from ERIM and NCIM

5.3 Non-steady state migration simulation based on "I" shape network

5.3.1 Influence of porosity

Figure 7 shows the comparison of simulated and predicted non-steady state migration coefficients development with porosity. In this simulation case, sizes of largest mother channel are fixed as: $d_0=w_0=l_0=1\mu m$, and step number (k) is equal to 10 according to Ref.[12]. The variance values obtained from this simulation are smaller than migration values in Figure 7; this implies that stable migration values are yielded. It is also found that the ion migration value increases with increase of the porosity [7]. This case may be explained as the

increase of pore space which provides transportation channels for ions [17]. A paste with longer hydration age usually has smaller porosity and thus presents lower ion diffusion/migration value. Besides, simulated results are generally consistent with ones predicted from fractal model, as illustrated in Figure 7.

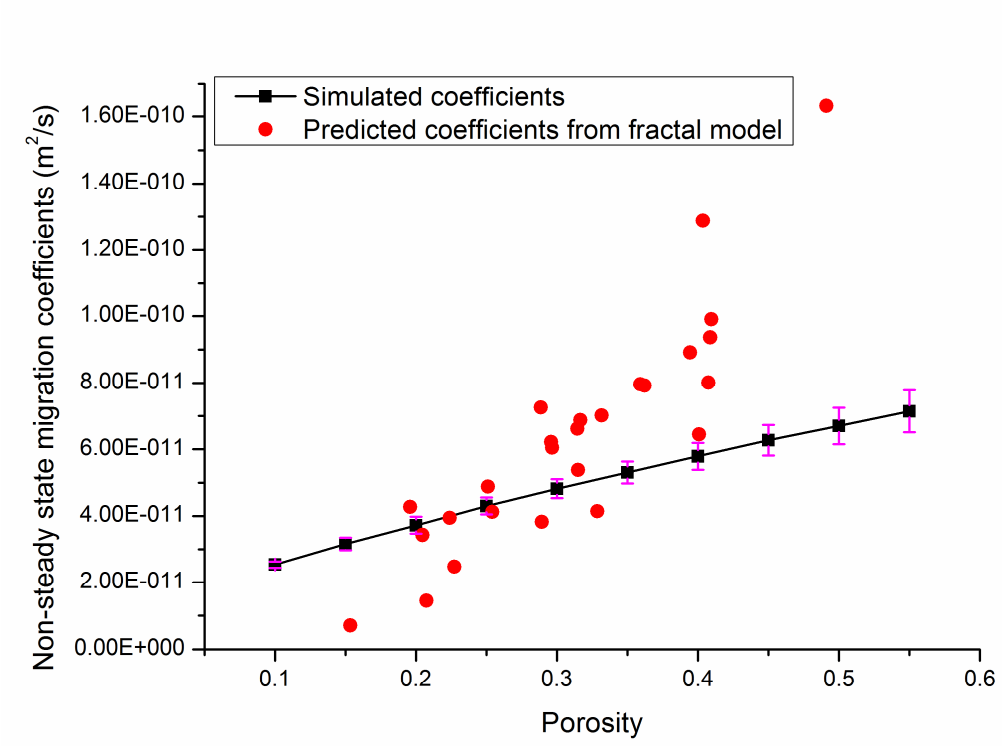

Fig.7. Comparison of simulated and predicted non-steady state migration coefficients development with porosity

5.3.2 Influence of diameter of largest mother channel

Figure 8 shows simulated non-steady state migration coefficients development with diameter of largest mother channel (d_0). The determination of actual diameter of largest mother

channel in complicated pore network of fractal saturated cement paste is practically somewhat difficult [9]. It is reported that d_0 in saturated cement paste may be associated with porosity, pore size distribution, solid phase imbibition coefficients and pore solution wetting properties [9]. As a consequence, for simplicity, d_0 is selected in wide range for this simulation, from 1 to 10μm with interval of 1μm, as shown in Figure 8, when other parameters of "I" shape network are kept as: w_0=l_0=1μm, k=10 and ϕ_c=0.3. It can be clearly observed that the non-steady state migration value doesn't present obvious fluctuation at given d_0 and steadily decreases from 13.09 to 4.81×10^{-11} m^2/s in the selected range of d_0 from 10 to 1 μm. It is expected that the dimension of large capillary pores in saturated cement pastes decreases naturally with hydration time and this will have a positive effect on the reduction of ion migration performance [9].

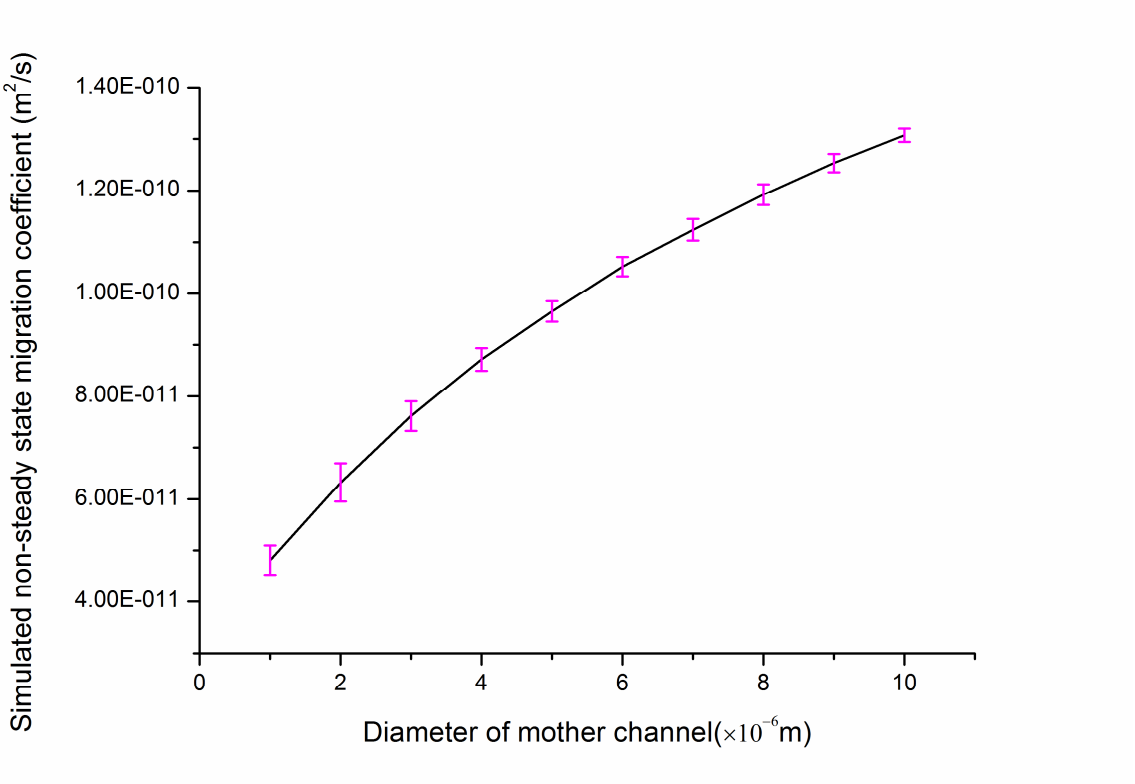

Fig.8. Simulated non-steady state migration coefficients development with diameter of largest mother channel

5.3.3 Influence of step number

Table 2 shows simulated non-steady state migration coefficients with different step numbers from 3 to 12 when $d_0=w_0=l_0=1\mu m$ and $\phi_c=0.3$. It can be seen that non-steady state ion migration value increases with small variance value as the step number of "I" shape network increases. As expected, the increase of step number will increase beyond doubt the number of small plentiful of transportation channels that is favorable for ion migration. In particular, it is also emphasized that migration coefficients tend to be stable as step number begins to reach to

353 9 in Table 2; this phenomenon may be explained that migration movements of ions are
354 strongly constrained by pore walls in small pores [24].

355 **Table 2** Simulated non-steady state migration coefficients with different step numbers

Step number	Non-steady state migration coefficient ($\times 10^{-11}$ m^2/s)	Variance ($\times 10^{-12}$ m^2/s)
3	4.48	1.67
4	4.62	1.99
5	4.68	2.03
6	4.71	2.41
7	4.75	2.55
8	4.79	2.64
9	4.82	2.73
10	4.82	2.84
11	4.82	2.95
12	4.82	2.95

356

357 ## 6. Conclusion

358 For the first time, this study presents a preliminary work to evaluate the diffusion and
359 migration of ions in fractal cement pastes at early age. The aggressive ion in this analysis is
360 taken as chloride ion that is widespread species in the marine environment. The traditional
361 migration test, electrical rapid ion migration (ERIM), has been carried out to assess the ability
362 of non-steady state ion migration $\left(D_{nssm}\right)$ in cement pastes at early age. Meanwhile, a newly

363 developed non-contact impedance measurement (NCIM) has been adopted in this work to in-
364 situ study the evolution of non-steady state ion migration coefficients in cement pastes
365 through a fractal model when ion binding capacity is considered. The corresponding non-
366 steady state ion migration coefficients predicted from the fractal model have good agreement
367 with ones measured by ERIM. Additionally, the influences of water to cement ratio, curing
368 hydration age, addition of fly ash, slag and silica fume on performance of ion migration in
369 cement paste can be observed obviously. A cement paste with lower water to cement ratio,
370 longer hydration age and addition of silica fume usually exhibits lower values of D_{nssm} due to
371 the reduction of pore space; on the contrary, addition of fly ash and slag is favorable to the
372 gain of values of D_{nssm}. NCIM combined with the proposed fractal model may have broad
373 prospects to predict the ion diffusion/migration performance of other porous media if the
374 fractal dimensions, ion binding capacity, minimal and maximal pore diameters can be
375 determined.

376 Besides, a fractal simulation based on an "I" shape network has been established to provide
377 valuable information of ion migration evolution with pore structure parameters in fractal
378 cement paste. It can be inferred that the simulated non-steady state ion migration coefficient
379 of fractal cement paste is associated with some structural parameters of "I" shape network,
380 such as size of largest mother channel and step number. From simulation results, it is shown
381 that larger porosity, diameter of largest mother channel or more step number of "I" shape
382 network is beneficial to yield larger values of D_{nssm}.

383 Indeed, the contribution of dead or isolated pores to ion diffusion/migration in fractal cement
384 pastes is not taken into consideration in this work since these pores have minor effect on the

385 transportation performance [24]. Additionally, some studies have been devoted to the
386 elucidation of the effect of temperature on the ion transportation performance in fractal porous
387 media [2, 26]. The resulting output in this work should be further optimized when the effect of
388 temperature on the transportation of ion diffusion/migration of cement pastes is clarified.

389

390 ## Acknowledgement

391 The support from the Hong Kong Research Grant Council under grant of 615412 and from
392 the China Ministry of Science and Technology under grant of 2009CB623200 is gratefully
393 acknowledged.

394 ## References

395 1. Z.J. Li, *Advanced concrete technology*, Wiley, Hoboken, N.J., 2011.

396 2. A.R. Stuart, P.K. Yuri and T.C. William, *Advances in Chemical Physics: Fractals,*
397 *Diffusion and Relaxation in Disordered complex system*, Wiley, Hoboken, N.J., 2006.

398 3. L.P. Tang, *Cem. Concr. Res.,* 1999,29, 1463-1468.

399 4. P. Spiesz and H.J.H. Brouwers, *Cem. Concr. Res.,* 2013,48, 116-127.

400 5. N. Narayanan and J. Jitendra, *Cem. Concr. Res.,* 2010,40, 1041-1051.

401 6. R. Deepak and N. Narayanan, *Cem. Concr. Res.,* 2013,44, 58-68.

402 7. R. Deepak and N. Narayanan, *Cem. Concr. Res.,* 2013,47, 31-42.

403 8. S.W. Tang, Z.J. Li, E. Chen and H.Y. Shao, *Constr. Build. Mater.,* 2013,51, 106-112.

404 9. S.W. Tang, Z.J. Li, H.G. Zhu, H.Y. Shao and E. Chen, *Constr. Build. Mater.,* 2014,59,
405 120-128.

406 10. Z.J. Li, S.W. Tang and Y.Y. Lu, *US Pat.,* 0158333 A1, 2012.

407 11. R. Francesca, F. Emiliano and B. Piero, *J. Phys. Chem. C.,* 2013,117, 25478-25487.

408 12. Q. Zheng, J. Xu, B. Yang and B. M. Yu, *Physica. A.,* 2013,392, 1557-1566.

409 13. M. Itagaki, S. Suzuki, I. Shitanda, K. Watanabe and H. Nakazawa, *J. Powers. Sources.,*
410 2007,164, 415-424.

411 14. M. Itagaki, Y. Hatada, I. Shitanda and K. Watanabe, *Electrochmi. Acta.,* 2010,55, 6255-
412 6262.

413 15. L.P. Tang, *Cem. Concr. Res.,* 1999,29, 1469-1474.

414 16. L.P. Tang and L.O. Nilsson, Proceedings of the 3rd RILEM workshop on Testing and
415 Modelling the Chloride Ingress into Concrete, Madrid,2002.

416 17. Q. Zheng, B.M. Yu, S.F. Wang and L. Luo, *Chem. Eng. Sci.,* 2012,68, 650-655.

417 18. L.Z. Xiao and Z.J. Li, *Cem. Concr. Res.,* 2008, 38, 312-319.

418 19. H.Y. Ma, Ph. D Thesis, The Hong Kong University of Science and Technology, 2013.

419 20. X.B. Jiang, J.K. Wang, B.K. Hou and G.H. He, *Ind. Eng. Chem. Res.,* 2013,52, 15685-
420 15701.

421 21. K. Rama, K. Rajesh and K.Y. Vivek, *J. Phys. Chem. C.,* 2008,112, 4019-4023.

422 22. L. Li and B.M. Yu, *Int. J. Heat. Mass. Transfer.,* 2013,67, 74-80.

423 23. K.B. Sanish, N. Narayanan and S. Manu, *Cem. Concr. Res.,* 2013, 49, 288-297.

424 24. K.K. Aligizaki, *Pore structure of cement-based materials: testing, interpretation, and*
425 *requirement*, Taylor & Francis, New York, 2006.

426 25. C.C. Yang and S.H. Weng, *Mater. Chem. Phys.,* 2011, 125, 876-882.

427 26. Q. Hu and J.S.Y. Wang, *Crit. Rev. Env. Sci. Tec.,* 2003, 33, 275-297.

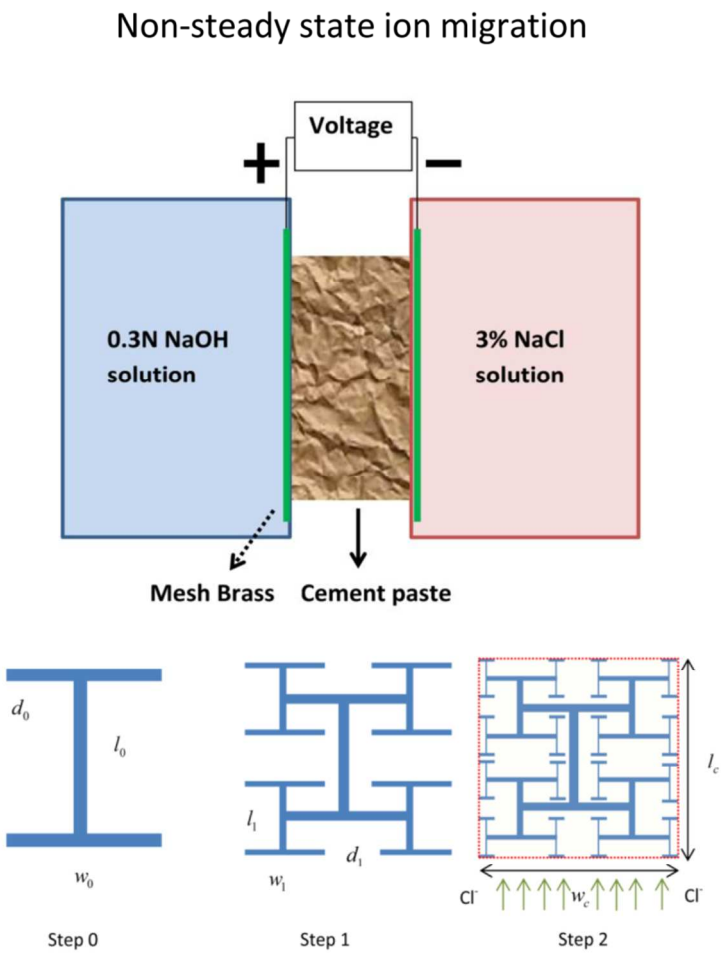

1) We have **theoretically** determined ions diffusion and migration coefficients in fractal porous media.

2) These coefficients of fractal cement pastes have been **experimentally** determined by ERIM and NCIM.

3) An innovative fractal network **simulation** for ion migration in fractal porous media has been established.